SCIENTIFIC ARTICLE

Influence of Brachial Plexus Birth Injury Location on Glenohumeral Joint Morphology

Nikhil N. Dixit, PhD,* Carolyn M. McCormick, MS,†‡ Jacqueline H. Cole, PhD,†‡ Katherine R. Saul, PhD*

Purpose Patient presentation after brachial plexus birth injury (BPBI) is influenced by nerve injury location; more contracture and bone deformity occur at the shoulder in postganglionic injuries. Although bone deformity after postganglionic injury is well-characterized, the extent of glenohumeral deformity after preganglionic BPBI is unclear.

Methods Twenty Sprague-Dawley rat pups received preganglionic or postganglionic neurectomy on a single forelimb at postnatal days 3 to 4. Glenohumeral joints on affected and unaffected sides were analyzed using micro–computed tomography scans after death at 8 weeks after birth. Glenoid version, glenoid inclination, glenoid and humeral head radius of curvature, and humeral head thickness and width were measured bilaterally.

Results The glenoid was significantly more declined in affected compared with unaffected shoulders after postganglionic ($-17.7° \pm 16.9°$) but not preganglionic injury. Compared with the preganglionic group, the affected shoulder in the postganglionic group exhibited significantly greater declination and increased glenoid radius of curvature. In contrast, the humeral head was only affected after preganglionic but not postganglionic injury, with a significantly smaller humeral head radius of curvature (-0.2 ± 0.2 mm), thickness (-0.2 ± 0.3 mm), and width (-0.3 ± 0.4 mm) on the affected side compared with the unaffected side; changes in these metrics were significantly associated with each other.

Conclusions These findings suggest that glenoid deformities occur after postganglionic BPBI but not after preganglionic BPBI, whereas the humeral head is smaller after preganglionic injury, possibly suggesting an overall decreased biological growth rate in this group.

Clinical relevance This study expands understanding of the altered glenoid and humeral head morphologies after preganglionic BPBI and its comparisons with morphologies after postganglionic BPBI. *(J Hand Surg Am. 2021;46(6):512.e1-e9. Copyright © 2021 by the American Society for Surgery of the Hand. All rights reserved.)*

Key words Brachial plexus birth injury, glenoid inclination, glenoid version, humeral head morphology, radius of curvature.

Online Exclusive

BRACHIAL PLEXUS BIRTH INJURY (BPBI) is the most common nerve injury among children,[1] most frequently affecting the C5-C6 nerve roots of the brachial plexus.[2] Although many children spontaneously recover nerve and muscle function, 20% to 30% of affected children do not have total

*From *Department of Mechanical and Aerospace Engineering, North Carolina State University, Raleigh; the †Joint Department of Biomedical Engineering, University of North Carolina, Chapel Hill; and the ‡North Carolina State University, Raleigh, NC.*

Received for publication June 25, 2019; accepted in revised form October 20, 2020.

No benefits in any form have been received or will be received related directly or indirectly to the subject of this article.

Corresponding author: Katherine R. Saul, PhD, Department of Mechanical and Aerospace Engineering, North Carolina State University, 911 Oval Drive, Campus Box 7910, Raleigh, NC 27695-7910; e-mail: ksaul@ncsu.edu.

0363-5023/21/4606-0012$36.00/0
https://doi.org/10.1016/j.jhsa.2020.10.019

neurological recovery.[3] Up to 33% of children affected with BPBI sustain permanent postural and osseous deformities,[4] which can have lifelong consequences for upper-limb function and quality of life.[5] Abnormal glenoid development, such as greater retroversion (posteriorly tilted glenoid face) and declination (inferiorly tilted glenoid face),[6–9] and increased humeral head flattening at the joint interface[10] are typical. Glenoid retroversion has been one of the notable changes observed in clinical studies,[6,11] but recent findings show that glenoid declination also contributes importantly to glenoid deformities.[7,12,13] The relative orientation of the bones is also affected; posterior humeral head subluxation is common.[6–9] These severe osseous deformities after BPBI affect function of the glenohumeral joint, causing dysplasia and joint subluxation.[14,15]

Brachial plexus birth injury presentation in patients can vary markedly according to the location of the nerve injury relative to the dorsal root ganglion. Nerve root ruptures, which occur distal to the ganglion (postganglionic), frequently result in paralysis with shoulder internal rotation and elbow flexion contractures.[16] In contrast, avulsion injuries proximal to the ganglion (preganglionic) typically result in paralysis without contractures at the shoulder and elbow.[17] Although surgical reconstruction can be indicated depending on the extent of bone deformity,[7,11] the relationship between the location of nerve injury (type of BPBI) and bone deformity is not well-described, but it could be useful for clinical decision-making. Clinical reports suggest that postural contractures significantly correlate with osseous deformities at the glenohumeral joint,[17] which implies that the extent of bone deformity may be related to nerve injury location. However, variability in patient condition (including the extent of nerve root involvement, completeness of nerve transection and recovery, and treatment history) can confound the ability to tease out direct relationships between nerve injury location and bone changes from the clinical record.[6,18] Because nerve injury can affect bone and joint development both directly (via neural regulation of bone remodeling)[19–23] and indirectly (via altered loading from changes in muscle or functional use),[12,18,24] isolating the effects of nerve injury location is a critical first step to understanding these contributions and developing improved treatments to prevent or reverse the bone deformity. Knowledge of the relative impact of innervation, passive muscle, and functional loading on ultimate deformity will allow clinicians to prioritize efforts better to reconstruct damaged nerves, relieve contractures, or normalize bone and joint loading.

Rat models of BPBI provide an opportunity to examine the effect of nerve injury location on bone growth in a controlled manner. Prior work showed that postganglionic rat models of BPBI exhibit shoulder neuromuscular anatomy[25] and bone deformities similar to those of human patients, including increased glenoid retroversion and declination[12,13,26] and smaller humeral head size.[26] However, quantitative bone changes with preganglionic BPBI have not been previously reported. A clearer understanding of patterns of bone changes with nerve injury is essential for a better understanding of the drivers of deformity formation as a foundation for understanding appropriate treatment targets and their effects. We conducted a study in a BPBI rat model to characterize the isolated effect of C5-C6 nerve injury location (preganglionic or postganglionic) on glenoid (version, inclination, and radius of curvature) and humeral head (thickness, width, and radius of curvature) morphology. We hypothesized that preganglionic injures would have less severe deformities compared with postganglionic injuries.

MATERIALS AND METHODS

All procedures were approved by the institutional animal care and use committee. We assigned 20 neonatal Sprague-Dawley rats to 2 injury groups: preganglionic ($n = 12$) and postganglionic ($n = 8$). The postganglionic group was from a previous study,[27] with an effect size of 1.7 for glenoid inclination angle changes and 1.2 for glenoid curvature changes. The sample size for the preganglionic group was chosen to detect an effect size of 1.8 ($\alpha = 0.05$ and power $= 0.8$). Neurectomies were performed under isoflurane anesthesia on pups at postnatal days 3-5. Preganglionic neurectomy was performed on the left forelimb, in which C5 and C6 nerve roots were excised proximal to the dorsal root ganglion via a supraclavicular incision, according to the methods of Nikolaou et al.[28] Postganglionic neurectomy was performed on the right forelimb, in which C5 and C6 nerve roots were excised distal to the dorsal root ganglion using a transverse infraclavicular incision through the pectoralis major muscle[26]; a prior publication[27] presented muscle measurements and glenoid version and inclination angles, without comparison with preganglionic injury. In the current study, we use computed tomography (CT) images obtained in the prior work to make new measurements of glenoid

and humeral bone shape, as described subsequently, and new comparisons with preganglionic measurements. After the procedures, incisions were closed with tissue adhesive and rat pups were given one prophylactic dose each of buprenorphine and carprofen. The rats were closely monitored for pain or distress; no additional analgesics were needed. All pups were kept with their respective dams for 3 weeks, weaned on postnatal day 21, and subsequently housed in shared cages with no more than 3 rats/cage. The animals were provided standard chow and water ad libitum. Body mass was measured every other day for 2 weeks after surgery and biweekly thereafter. At 8 weeks of age, animals were killed via CO_2 asphyxiation followed by bilateral thoracotomy. Upon death, the upper torso was separated from the body with a guillotine and skin was removed; the torso was then fixed in 10% neutral buffered formalin for 2 days at room temperature and stored in 70% ethanol at 4°C. Before micro-CT, all upper-limb muscles were dissected, but the glenohumeral joint was kept intact with the scapula and humeral head attached to each other.

To evaluate glenohumeral morphology, affected and unaffected intact shoulder joints (connected humerus and scapula) for preganglionic rats were imaged with micro-CT (SCANCO μCT 80, Brüttisellen, Switzerland), using an x-ray energy of 70 kVp at 114 μA, 800 ms of integration time, 1,000 projections/rotation, no frame averaging, and a 0.5-mm Al filter. Samples were scanned in 70% ethanol; the scans were reconstructed at an isotropic voxel size of 36 μm. Existing micro-CT scans for the postganglionic group[27] were evaluated for comparison. Right (affected) and left (unaffected) scapulae and humeri for both preganglionic and postganglionic groups were segmented in Mimics software (Materialise, Leuven, Belgium), and each bone image was thresholded such that bone surface details were captured accurately. Morphological measurements were made from the 3-dimensional (3D) surfaces, including glenoid version angle, glenoid inclination angle, glenoid radius of curvature, humeral head radius of curvature, humeral head thickness, and humeral head width. Glenoid version angle was defined in the transverse plane of the scapula in which the glenoid was widest, measured as the angle complementary to the angle between the plane of the scapular body and the tangent to the glenoid rim (Fig. 1A). The glenoid inclination angle was defined in a local scapular plane, measured as the complementary angle to the angle between the scapular spine and the glenoid rim tangent (Fig. 1B). The glenoid (Fig. 1C) and humeral head radius of curvature (Fig. 2B) were measured in the same plane as the glenoid inclination angle by fitting a circle to the respective articular surfaces. The humeral head thickness (epiphyseal depth) and width were defined in the same plane as the glenoid inclination angle by fitting an ellipse to the humeral head and measuring the major radius and minor diameter of the ellipse, respectively (Fig. 2A). The width axis of the ellipse was aligned along a line approximately parallel to the medial region of the growth plate and intersecting with the center of the growth plate, and the thickness axis was defined perpendicular to the width axis. For the postganglionic group, the glenoid version and inclination angles were previously analyzed and reported,[27] as described earlier. The new humeral head and glenoid radius of curvature measurements made from the existing CT images (and new comparisons of all measurements with preganglionic morphology) are described here.

We evaluated the normality of the data for each metric using Shapiro-Wilk tests. Morphological measurements of the glenoid and humeral head were compared between the affected and the unaffected limb within each injury group (preganglionic and postganglionic) using paired t tests for normally distributed data and Wilcoxon signed rank tests for nonnormal data. Comparisons between the preganglionic and postganglionic injury groups were performed based on the difference between the affected and unaffected side for each morphological metric using either unpaired t tests (if normally distributed) or Mann-Whitney U tests (if nonnormal). All comparisons used a significance level of $\alpha = 0.05$.

RESULTS

All data were normally distributed, except for humeral head thickness in the unaffected limb of the preganglionic group and the difference in glenoid version between the affected and unaffected side in the postganglionic group. In the preganglionic group, the glenoid retroversion (difference = $-1.3° \pm 4.7°$) and declination ($-1.2° \pm 9.5°$) (Fig. 3) were not significantly different in the affected limb relative to the unaffected limb. In the postganglionic group, the affected glenoid had significantly more declination ($-17.7° \pm 16.9°$; $P < .05$) relative to the unaffected glenoid (Fig. 3). The glenoid radius of curvature was not significantly different on the affected side relative to the unaffected side in the

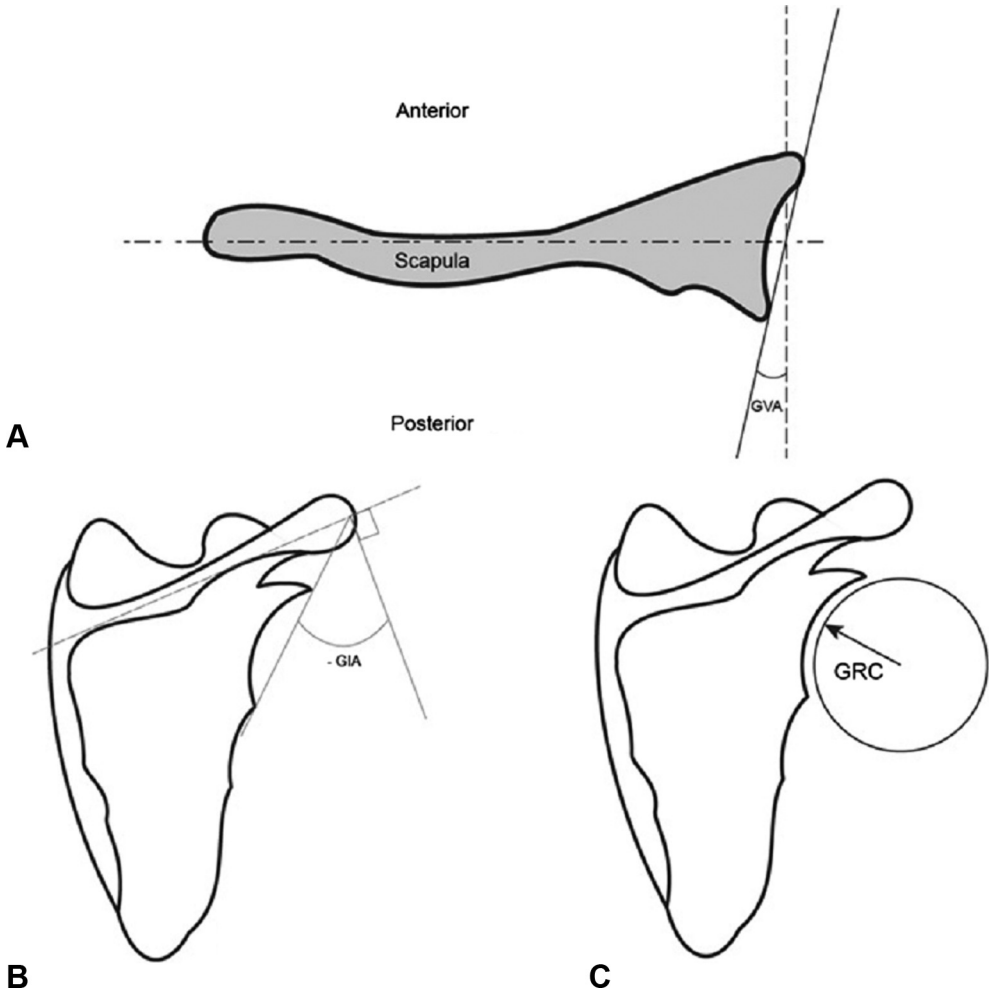

FIGURE 1: Glenoid morphology measures. **A** The glenoid version angle (GVA) was defined in the transverse plane of the scapula in which the glenoid was widest, measured as the angle complementary to the angle between the plane of the scapular body and the tangent to the glenoid rim. **B** The glenoid inclination angle (GIA) was defined in a local scapular plane, measured as the complementary angle to the angle between the scapular spine and the glenoid rim tangent. **C** The glenoid radius of curvature (GRC) was measured in the same plane as the GIA by fitting a circle to the articular surface. For the postganglionic group, GVA and GIA were previously analyzed and reported.[27]

preganglionic group (−0.1 ± 0.5 mm) (Fig. 4). When comparing injury groups, the glenoid exhibited significantly higher declination ($P < .05$) and curvature ($P < .05$) for the postganglionic group than for the preganglionic group.

In the preganglionic group, the affected side had a significantly smaller humeral head radius of curvature (-0.2 ± 0.2 mm, $p < 0.05$) (Fig. 4), thickness (-0.2 ± 0.3 mm, $p < 0.05$), and width −-0.3 ± 0.4 mm; $P < .05$) (Fig. 5) compared with the unaffected side. In the postganglionic group, humeral head morphology did not differ significantly between the 2 limbs for curvature (−0.1 ± 0.5 mm) (Fig. 4) or humeral head thickness (−0.3 ± 0.6 mm) and width (−0.2 ± 0.4 mm) (Fig. 5). Comparing injury groups, no significant differences were observed between postganglionic and preganglionic groups for humeral head radius of curvature, thickness, or width.

DISCUSSION

Glenohumeral morphology was markedly affected by neonatal injury to the brachial plexus, and the effects were significantly influenced by the location of the injury relative to the dorsal root ganglion. Glenoid morphology was more altered after postganglionic injury, with severe glenoid declination. The affected glenoid declination in the postganglionic group (difference between limbs, −17.7° ± 16.9°) was consistent with reports of declination after BPBI in humans (median difference between limbs, −15.0°).[7] Glenoid retroversion in the postganglionic group

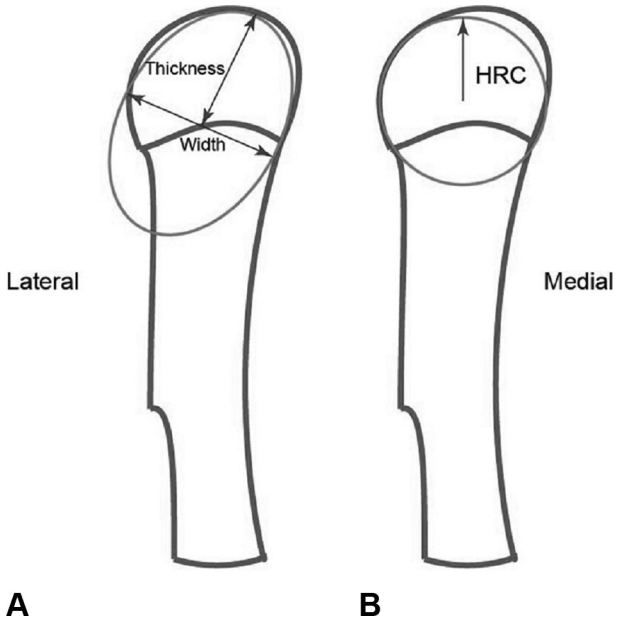

FIGURE 2: Humeral head morphology measures. **A** The humeral head thickness and width were defined in the same plane as the glenoid inclination angle by fitting an ellipse to the humeral head and measuring the major radius and minor diameter of the ellipse, respectively. **B** The humeral head radius of curvature (HRC) was measured in the same plane as glenoid inclination angle by fitting a circle to the articular surface.

(difference between limbs, −7.4° ± 11.4°) was also similar to values observed in humans (difference between limbs, −10.2° ± 11.6°) in prior work examining 102 children after BPBI.[11] Increased glenoid radius of curvature after postganglionic injury reflects flattening of the glenoid surface, which represents a meaningful alteration to joint function, because glenoid curvature is essential for maintaining shoulder stability.[29] We found no evidence of altered glenoid version, declination, or radius of curvature in the affected limb relative to the unaffected limb for the preganglionic group. Taken together, these observations suggest that glenoid deformity is severe only after postganglionic C5-C6 injury. Although most clinical studies describing bone deformity do not specifically report whether ruptures or avulsions are present, the current results are consistent with prior clinical reports of glenoid deformities,[6,10,11,30] which include primarily patients with Narakas level I and II injuries, and describe more severe changes to the glenoid with Narakas level I injuries.[11]

In contrast, humeral head morphology was more altered after preganglionic injury. The overall size of the humeral head was markedly smaller, with a smaller radius of curvature, thickness, and width after preganglionic injury, but no significant changes were detected to the humeral head after postganglionic injury. A prior study in rats reported that humeral head width and thickness tended to be smaller after postganglionic injury,[13] in contrast to our findings, but that study did not assess the radius of curvature. Consistent with our study, a clinical report on children with BPBI described smaller humeral head features and overall osseous atrophy on the affected arm.[31] Although this clinical report does not explicitly describe the preganglionic or postganglionic nature of the injuries, the patients as a group are described as having Narakas scores with an average of 2.5 (SD ± 0.8); a Narakas level of II corresponds to injury of C5-C7 roots with spontaneous recovery in approximately 60% of patients whereas Narakas level III corresponds to effects for C5-T1 levels and a complete flaccid paralysis with no Horner syndrome, and recovery in only 30% to 50% of patients.[32]

Because bone growth is driven by both mechanical and biological factors,[33] differences in bone development after preganglionic and postganglionic injury may be driven by differences in both joint loading and biological stimulus in the 2 presentations. For example, evidence in young rats suggests that bone innervation has a direct impact on bone remodeling, such as temporal and spatial matching of sensory nerves with active bone sites.[34] After spinal cord injury, bone loss exceeds that which can be fully explained by unloading from disuse alone,[35,36] and rapid bone loss even with muscle stimulation after spinal cord injury supports a direct neurologic−bone connection.[37,38] Mechanical loading of bone tissue is influenced by joint forces induced by muscle loading as well as limb use. Postganglionic injury is frequently associated with muscle contractures that cause restriction in shoulder external rotation,[6,8,18] causing high passive muscle forces acting on the bone. These observations in the clinical population are corroborated by work in rat and mouse models of BPBI, in which restricted muscle growth in length and increased contracture are reported.[12,28] Computational models of BPBI suggest that this reduced muscle growth in length would mechanically result in both restricted range of motion and altered glenoid loading consistent with the observed deformity after postganglionic neurectomy.[12,39] However, in both clinical and animal studies, contractures are minimal after preganglionic injuries[17,40]; thus, only low joint forces from reduced limb use and muscle paralysis are present. Therefore, glenoid differences may be primarily driven by differences in joint load. However, in contrast to the postganglionic case, in the absence of marked contracture after preganglionic injury, altered

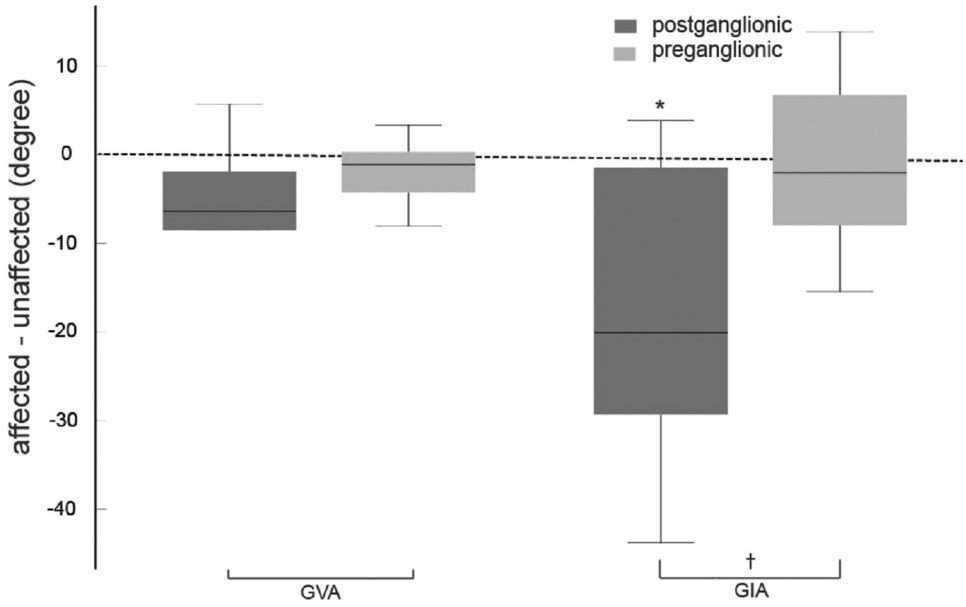

FIGURE 3: The glenoid version and inclination angles (GVA and GIA, respectively) are shown. The glenoid was significantly more declined on the affected limb compared with the unaffected limb in postganglionic injuries. The difference in affected limb GIA relative to the unaffected limb differed between the 2 injury groups, with higher relative declination in the postganglionic group compared with the preganglionic group. *$p < 0.05$ for the affected versus unaffected limb. †$p < 0.05$ for the preganglionic versus postganglionic injury group. For the postganglionic group, GVA and GIA were previously analyzed and reported.[27]

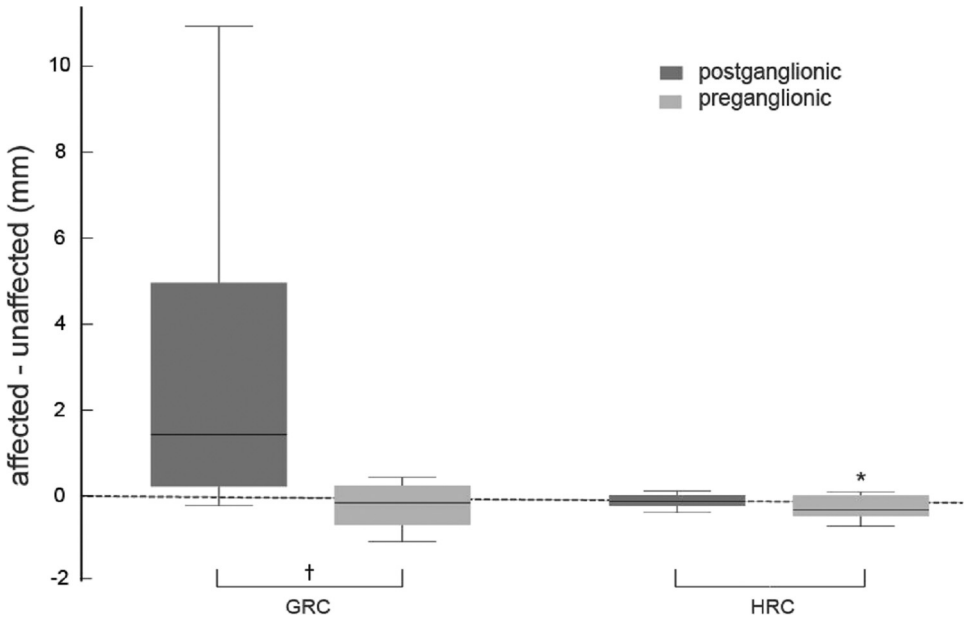

FIGURE 4: Glenoid and humeral head curvature (GRC and HRC, respectively) are shown. The difference in the affected limb GRC relative to the unaffected limb differed between the 2 injury groups, with the postganglionic injuries exhibiting larger relative GRC than the preganglionic group. The HRC was significantly smaller on the affected side compared with the unaffected side after preganglionic injury. *$p < 0.05$ for the affected versus unaffected limb. †$p < 0.05$ for the preganglionic versus postganglionic injury group.

biological signals caused by the nerve injury or reduced limb use may dominate the changes in bone growth, leading to overall slower bone formation and smaller bones. Clinical and other animal BPBI studies have also reported smaller humeral and scapular geometry,[13,31] providing additional evidence for reduced biological growth after nerve injury. Thus, when examined in the context of the literature, this work

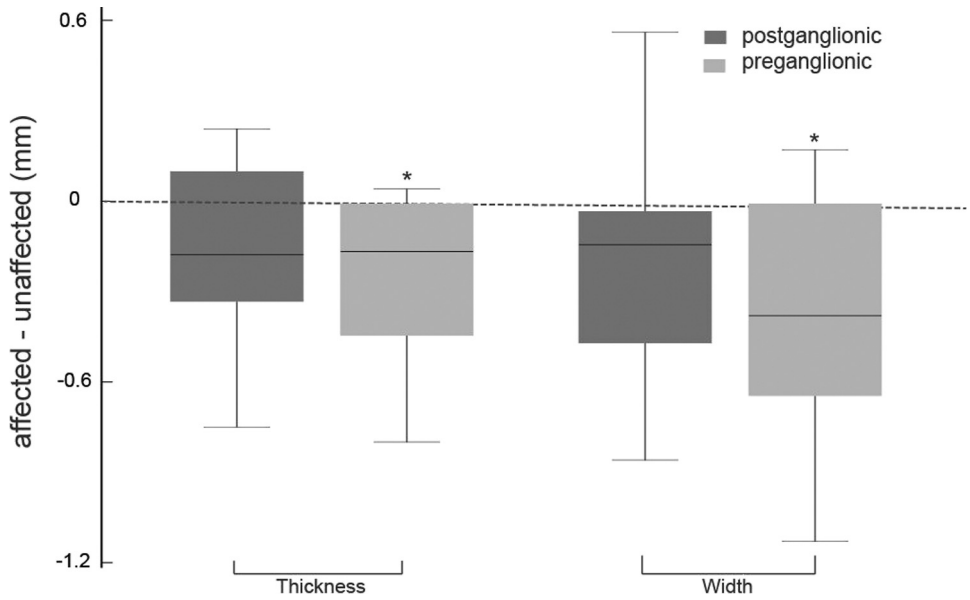

FIGURE 5: Humeral head dimensions. The humeral head was significantly smaller in thickness and width in the preganglionic affected limb compared with the unaffected limb. The postganglionic group did not exhibit significant changes in humeral head thickness or width in the affected limb. *$p < 0.05$ for the affected versus unaffected limb.

provides support that glenoid shape deformities, seen more in the postganglionic case, are likely to be driven by the presence of contracture and high passive muscle forces, whereas humeral deficiencies after preganglionic injury are more likely to be driven by reduced limb use and direct nerve injury.

Surgical approaches are often used to correct the shoulder dislocation and severe dysplasia and joint subluxation that are a consequence of the glenohumeral deformity after BPBI.[15] Specific techniques include anterior translation of the humeral head to prevent dislocation,[41] external rotation tendon transfer,[7] or glenoid osteoplasty or osteotomy,[14] Surgical decisions are typically planned based on axial plane measures,[30,42] especially glenoid retroversion, which do not account for coronal or sagittal plane changes, and which may be confounded by imaging plane and scapular positioning.[43] However, recent 3D medical imaging reconstructions of glenoid geometry in BPBI patients, in which true glenoid angles can be extracted, rather than planar projections that may be affected by plane selection, suggest that glenoid declination may also be greatly altered after nerve rupture (postganglionic injury).[44] Our study using 3D imaging corroborates that glenoid declination is also a key marker in characterizing glenoid deformity in this animal model. However, our work also suggests that glenohumeral deformity depends heavily on BPBI location, which may provide an additional foundation on which surgical decision-making can be informed.

The results of the current study should be evaluated in light of its limitations. Although nerve excision was evaluated and confirmed by observing the phenotype after the surgical procedure, spontaneous recovery of the nerve injury can occur and may contribute to the variability that was observed within groups.[4] The existing animal models on which this study relied were validated using transection as a surrogate for complete rupture or avulsion, but not for partial injuries.[26,45] Because complete nerve injuries are more likely to result in marked bone or postural deformities,[17] and there are limited data quantifying preganglionic and postganglionic bone deformities, our primary focus for this study was to quantify the extent of bone deformities after complete injuries. Future work should consider the effect of partial lesions and explore the use of animal models for partial injury and their effects on muscle and bone. Although rat neuromuscular anatomy is similar to that of humans,[25] mechanical loading of the glenohumeral joint may differ between species, because rats experience lifelong quadrupedal loading, whereas human infants do so only during the first year.[12] Bone deformity was investigated at only one time point (8 weeks after birth) for both injury groups, and by this time shoulder deformity is well-established in this model.[12,13,26] The growth of the humeral head or

scapular glenoid over 8 weeks in the rat is equivalent to 5.8 human years[12,46]; skeletal maturity in rats is reached at approximately 20 weeks.[47] To measure the glenohumeral joint features, clinical studies used a minimum age for patients of 3 years to allow enough time for bone ossification so that metrics could be adequately assessed.[6] Thus, for rats in this study, we used an 8-week time point to ensure the deformity was established and adequate ossification of the bone had occurred. However, assessing injury progression over time will be critical in future work to understand the timing of deformity initiation and inform optimal treatment timing. In this study, we do not report other metrics that relate to the congruence and alignment of the humerus relative to the glenoid, such as percent coverage, percent humeral head displacement, or percent humeral head anterior to scapular axis. These measures typically require measurements from an intact shoulder.[48,49] However, the current study required high-resolution micro-CT scans to be acquired of the scapula and humerus individually after dissection; thus, these metrics were not captured. However, in prior work by our group,[12] alignment of the humeral head relative to the glenoid was reported for postganglionic injury.

Our humeral head measurements of width and height are similar to those previously reported by Li et al,[13] who also observed smaller humeral head features on the affected rats. The humeral head measures in this study have not been described in clinical studies. Sheehan et al[31] described a smaller humeral head in humans, but our metrics are different because the study by Sheehan et al provided metrics from the entire humerus, which we did not analyze in this work.

The current work highlights changes in bone and provides quantification of bone morphology after preganglionic injury, adding to previously reported changes after postganglionic injury. The study also provides essential comparisons of morphological changes between preganglionic and postganglionic injury, which are needed to isolate contributions of the biological and mechanical consequences of nerve injury to bone and joint development. Understanding the interactions of innervation, passive muscle loading, and functional limb loading during musculoskeletal growth and deformity development with BPBI will aid clinicians in decisions on treatment type (eg, nerve reconstruction, contracture relief, or normalized bone or joint loading) and timing. To understand these interactions, measures of muscle and limb function are also essential; prior and ongoing work of our group[40] and others[28] explore those factors. Computational work[39] and other clinical conditions also suggest that differences in bone morphology likely reflect differences in mechanical loading from altered muscle and disuse, which may be an important consideration for developing treatments to preserve the articulating geometry.

This study clearly identified differences in glenohumeral osseous deformities after preganglionic and postganglionic BPBI. Glenoid deformities were more severe after postganglionic injury, with a markedly altered shape profile, whereas changes in humeral head morphology were more pronounced after preganglionic injury, with an overall smaller head. A clearer understanding of bone change patterns with nerve injury provides an important foundation for future work to understand better the drivers of deformity formation.

ACKNOWLEDGMENTS

This study was funded by National Institutes of Health Grant R21 HD088893. Contributions from Dr Roger Cornwall, Dr Kerry Danelson, and Dr Thomas Smith were made in performing preganglionic and postganglionic neurectomies.

REFERENCES

1. Foad SL, Mehlman CT, Ying J. The epidemiology of neonatal brachial plexus palsy in the United States. *J Bone Joint Surg Am*. 2008;90(6):1258–1264.
2. Lagerkvist AL, Johansson U, Johansson A, Bager B, Uvebrant P. Obstetric brachial plexus palsy: a prospective, population-based study of incidence, recovery, and residual impairment at 18 months of age. *Dev Med Child Neurol*. 2010;52(6):529–534.
3. Pondaag W, Malessy MJ, van Dijk JG, Thomeer RT. Natural history of obstetric brachial plexus palsy: a systematic review. *Dev Med Child Neurol*. 2004;46(2):138–144.
4. Pearl ML. Shoulder problems in children with brachial plexus birth palsy: evaluation and management. *J Am Acad Orthop Surg*. 2009;17(4):242–254.
5. Bae DS, Waters PM, Zurakowski D. Correlation of pediatric outcomes data collection instrument with measures of active movement in children with brachial plexus birth palsy. *J Pediatr Orthop*. 2008;28(5):584–592.
6. Bhardwaj P, Burgess T, Sabapathy SR, Venkataramani H, Ilayaraja V. Correlation between clinical findings and CT scan parameters for shoulder deformities in birth brachial plexus palsy. *J Hand Surg Am*. 2013;38(8):1557–1566.
7. Eismann EA, Laor T, Cornwall R. Three-dimensional magnetic resonance imaging of glenohumeral dysplasia in neonatal brachial plexus palsy. *J Bone Joint Surg Am*. 2016;98(2):142–151.
8. Eismann EA, Little KJ, Laor T, Cornwall R. Glenohumeral abduction contracture in children with unresolved neonatal brachial plexus palsy. *J Bone Joint Surg Am*. 2015;97(2):112–118.
9. van Gelein Vitringa VM, van Royen BJ, van der Sluijs JA. Scapular deformity in obstetric brachial plexus palsy and the Hueter-Volkmann law: a retrospective study. *BMC Musculoskelet Disord*. 2013;14:107.

10. Sibinski M, Wozniakowski B, Drobniewski M, Synder M. Secondary gleno-humeral joint dysplasia in children with persistent obstetric brachial plexus palsy. *Int Orthop*. 2010;34(6):863−867.
11. Hogendoorn S, van Overvest KL, Watt I, Duijsens AH, Nelissen RG. Structural changes in muscle and glenohumeral joint deformity in neonatal brachial plexus palsy. *J Bone Joint Surg Am*. 2010;92(4):935−942.
12. Cheng W, Cornwall R, Crouch DL, Li Z, Saul KR. Contributions of muscle imbalance and impaired growth to postural and osseous shoulder deformity following brachial plexus birth palsy: a computational simulation analysis. *J Hand Surg Am*. 2015;40(6):1170−1176.
13. Li Z, Barnwell J, Tan J, Koman LA, Smith BP. Microcomputed tomography characterization of shoulder osseous deformity after brachial plexus birth palsy: a rat model study. *J Bone Joint Surg Am*. 2010;92(15):2583−2588.
14. Di Mascio L, Chin KF, Fox M, Sinisi M. Glenoplasty for complex shoulder subluxation and dislocation in children with obstetric brachial plexus palsy. *J Bone Joint Surg Br*. 2011;93(1):102−107.
15. Kambhampati SB, Birch R, Cobiella C, Chen L. Posterior subluxation and dislocation of the shoulder in obstetric brachial plexus palsy. *J Bone Joint Surg Br*. 2006;88(2):213−219.
16. Waters PM. Update on management of pediatric brachial plexus palsy. *J Pediatr Orthop B*. 2005;14(4):233−244.
17. Al-Qattan MM. Obstetric brachial plexus palsy associated with breech delivery. *Ann Plast Surg*. 2003;51(3):257−264 [discussion: 265].
18. Pearl ML, Edgerton BW. Glenoid deformity secondary to brachial plexus birth palsy. *J Bone Joint Surg Am*. 1998;80(5):659−667.
19. Garcia-Castellano JM, Diaz-Herrera P, Morcuende JA. Is bone a target-tissue for the nervous system? New advances on the understanding of their interactions. *Iowa Orthop J*. 2000;20:49−58.
20. Grässel SG. The role of peripheral nerve fibers and their neurotransmitters in cartilage and bone physiology and pathophysiology. *Arthritis Res Ther*. 2014;16(6):485.
21. Huang S, Li Z, Liu Y, et al. Neural regulation of bone remodeling: Identifying novel neural molecules and pathways between brain and bone. *J Cell Physiol*. 2019;234(5):5466−5477.
22. Jones KB, Mollano AV, Morcuende JA, Cooper RR, Saltzman CL. Bone and brain: a review of neural, hormonal, and musculoskeletal connections. *Iowa Orthop J*. 2004;24:123−132.
23. Lerner UH. Neuropeptidergic regulation of bone resorption and bone formation. *J Musculoskelet Neuronal Interact*. 2002;2(5):440−447.
24. Crouch DL, Plate JF, Li Z, Saul KR. Computational sensitivity analysis to identify muscles that can mechanically contribute to shoulder deformity following brachial plexus birth palsy. *J Hand Surg Am*. 2014;39(2):303−311.
25. Norlin R, Hoe-Hansen C, Oquist G, Hildebrand C. Shoulder region of the rat: anatomy and fiber composition of some suprascapular nerve branches. *Anat Rec*. 1994;239(3):332−342.
26. Li Z, Ma J, Apel P, Carlson CS, Smith TL, Koman LA. Brachial plexus birth palsy-associated shoulder deformity: a rat model study. *J Hand Surg Am*. 2008;33(3):308−312.
27. Crouch DL, Hutchinson ID, Plate JF, et al. Biomechanical basis of shoulder osseous deformity and contracture in a rat model of brachial plexus birth palsy. *J Bone Joint Surg Am*. 2015;97(15):1264−1271.
28. Nikolaou S, Hu L, Cornwall R. Afferent innervation, muscle spindles, and contractures following neonatal brachial plexus injury in a mouse model. *J Hand Surg Am*. 2015;40(10):2007−2016.
29. Flatow EL, Cuomo F, Maday MG, Miller SR, McIlveen SJ, Bigliani LU. Open reduction and internal fixation of two-part displaced fractures of the greater tuberosity of the proximal part of the humerus. *J Bone Joint Surg Am*. 1991;73(8):1213−1218.
30. Waters PM, Smith GR, Jaramillo D. Glenohumeral deformity secondary to brachial plexus birth palsy. *J Bone Joint Surg Am*. 1998;80(5):668−677.
31. Sheehan FT, Brochard S, Behnam AJ, Alter KE. Three-dimensional humeral morphologic alterations and atrophy associated with obstetrical brachial plexus palsy. *J Shoulder Elbow Surg*. 2014;23(5):708−719.
32. Al-Qattan MM, El-Sayed AA, Al-Zahrani AY, et al. Narakas classification of obstetric brachial plexus palsy revisited. *J Hand Surg Eur Vol*. 2009;34(6):788−791.
33. Giorgi M, Carriero A, Shefelbine SJ, Nowlan NC. Mechanobiological simulations of prenatal joint morphogenesis. *J Biomech*. 2014;47(5):989−995.
34. Gajda M, Litwin JA, Cichocki T, Timmermans JP, Adriaensen D. Development of sensory innervation in rat tibia: co-localization of CGRP and substance P with growth-associated protein 43 (GAP-43). *J Anat*. 2005;207(2):135−144.
35. Jiang SD, Jiang LS, Dai LY. Mechanisms of osteoporosis in spinal cord injury. *Clin Endocrinol (Oxf)*. 2006;65(5):555−565.
36. Leblanc AD, Schneider VS, Evans HJ, Engelbretson DA, Krebs JM. Bone mineral loss and recovery after 17 weeks of bed rest. *J Bone Miner Res*. 1990;5(8):843−850.
37. Bickel CS, Slade JM, Haddad F, Adams GR, Dudley GA. Acute molecular responses of skeletal muscle to resistance exercise in able-bodied and spinal cord-injured subjects. *J Appl Physiol (1985)*. 2003;94(6):2255−2262.
38. Maimoun L, Couret I, Micallef JP, et al. Use of bone biochemical markers with dual-energy x-ray absorptiometry for early determination of bone loss in persons with spinal cord injury. *Metabolism*. 2002;51(8):958−963.
39. Dixit NN, McFarland DC, Saul KR. Computational analysis of glenohumeral joint growth and morphology following a brachial plexus birth injury. *J Biomech*. 2019;86:48−54.
40. Dixit NN, McCormick CM, Warren E, Cole JH, Saul KR. Preganglionic and postganglionic brachial plexus birth injury effects on shoulder muscle growth. *J Hand Surg Am*. 2021;46(2):146.e1−146.e9.
41. Waters PM, Monica JT, Earp BE, Zurakowski D, Bae DS. Correlation of radiographic muscle cross-sectional area with glenohumeral deformity in children with brachial plexus birth palsy. *J Bone Joint Surg Am*. 2009;91(10):2367−2375.
42. Lippert WC, Mehlman CT, Cornwall R, et al. The intrarater and interrater reliability of glenoid version and glenohumeral subluxation measurements in neonatal brachial plexus palsy. *J Pediatr Orthop*. 2012;32(4):378−384.
43. Stein J, Laor T, Carr P, Zbojniewicz A, Cornwall R. The effect of scapular position on magnetic resonance imaging measurements of glenohumeral dysplasia caused by neonatal brachial plexus palsy. *J Hand Surg Am*. 2017;42(12):1030.e1−1030.e11.
44. Brochard S, Mozingo JD, Alter KE, Sheehan FT. Three dimensionality of gleno-humeral deformities in obstetrical brachial plexus palsy. *J Orthop Res*. 2016;34(4):675−682.
45. Kim HM, Galatz LM, Das R, Patel N, Thomopoulos S. Musculoskeletal deformities secondary to neurotomy of the superior trunk of the brachial plexus in neonatal mice. *J Orthop Res*. 2010;28(10):1391−1398.
46. Quinn R. Comparing rat's to human's age: how old is my rat in people years? *Nutrition*. 2005;21(6):775−777.
47. Horton JA, Bariteau JT, Loomis RM, Strauss JA, Damron TA. Ontogeny of skeletal maturation in the juvenile rat. *Anat Rec (Hoboken)*. 2008;291(3):283−292.
48. Bauer AS, Lucas JF, Heyrani N, Anderson RL, Kalish LA, James MA. Ultrasound screening for posterior shoulder dislocation in infants with persistent brachial plexus birth palsy. *J Bone Joint Surg Am*. 2017;99(9):778−783.
49. Donohue KW, Little KJ, Gaughan JP, Kozin SH, Norton BD, Zlotolow DA. Comparison of ultrasound and MRI for the diagnosis of glenohumeral dysplasia in brachial plexus birth palsy. *J Bone Joint Surg Am*. 2017;99(2):123−132.